Progress In Electromagnetics Research, Vol. 142, 309–320, 2013

NOVEL DESIGN OF A COMPACT TRIPLE-BAND BANDPASS FILTER USING SHORT STUB-LOADED SIRS AND EMBEDDED SIRS STRUCTURE

Kaida Xu[1, 2, *], Yonghong Zhang[1], Daotong Li[1], Yong Fan[1], Joshua Le-Wei Li[3], William T. Joines[2], and Qing Huo Liu[2]

[1]EHF Key Lab of Fundamental Science, University of Electronic Science and Technology of China, Chengdu 611731, China

[2]Department of Electrical and Computer Engineering, Duke University, Durham, NC 27708, USA

[3]Institute of Electromagnetics, University of Electronic Science and Technology of China, Chengdu 611731, China

Abstract—A novel compact planar triple-band bandpass filter using two sets of short stub-loaded stepped impedance resonators (SSLSIRs) and a pair of embedded stepped impedance resonators (ESIRs) has been proposed. The SSLSIRs can adjust the bandwidths of the corresponding passbands over a wide range, and the ESIRs employing non 0°-feed coupled structure with mixed electric and magnetic coupling can obtain an extra transmission zero. The embedded resonators structure can further miniaturize the dimensions of the whole triple-band filter. The operating frequencies of the SSLSIRs and ESIRs are designed for the applications of the WLAN (2.45/5.2 GHz) and WiMAX (3.5 GHz) systems, respectively. The simulated and measured results are both presented and show good agreement.

1. INTRODUCTION

Due to low cost and convenient integration, planar microstrip multiple-band bandpass filters (BPFs) have been widely explored to satisfy concurrently multiple microwave and wireless communication systems such as GSM (0.9/1.8 GHz), WiMAX (3.5 GHz) and WLAN (2.4/5.2 GHz) applications. A variety of approaches to design

Received 5 August 2013, Accepted 28 August 2013, Scheduled 5 September 2013

* Corresponding author: Kaida Xu (kx10@duke.edu).

microstrip dual-band or multi-band bandpass filters have been proposed [1–9]. One of the methods to achieve multi-band response with compact size and high performance is to employ the stepped impedance resonators (SIRs) [8–10]. In 1979, Makimoto and Yamashita [11] created SIR technique for the design of compact and high-Q bandpass filters. From then on, a multitude of improved bandpass filters based on SIRs have been developed [12–17]. Using the method of the odd- and even-mode analysis, the open or short stub-loaded resonators (SLRs) are another new and useful structures to design dual-band and even multi-band filters [18–24]. In [18], a dual-band BPF using open stub-loaded resonator (OSLR) and 0° feeding structure was first analyzed and designed. Moreover, the short stub-loaded resonator (SSLR) was also analyzed in [19] for design of compact bandpass filter. In [22], a multi-mode multi-band filter using both short and open stub-loaded resonator was proposed to make the size more compact. Furthermore, a new tri-band filter with combined SIR and OSLR structures was analyzed and discussed [10]. However, the bandwidths of three passbands were hardly adjusted over a wide range.

To miniaturize the dimensions of the overall structure, the embedded resonator was explored and developed. A dual-feeding structure with embedded resonators was employed to design a compact dual-band filter [2]. In [4], two sets of spiral-lines were embedded in the rectangular open loops to obtain the embedded spiral resonators. These embedded-shaped structures could greatly reduce the overall size and make the filter much more compact.

In this paper, we proposed and analyzed a novel miniaturized planar microstrip tri-band BPF using two sets of SSLSIRs and a pair of ESIRs with a direct-coupled feeding structure. The proposed filter with three passbands is centered at 2.45/3.5/5.2 GHz for combination of WiMAX (3.5 GHz) and WLAN (2.45/5.2 GHz) applications. Meanwhile, the proposed filter has compact circuit size and strong design flexibility since it is implemented with three parallel transmission paths for three specific passbands and easily determined by tuning the parameters of each resonator, which is convenient to design each single-band independently.

2. RESONATOR ANALYSIS OF THE TRI-BAND BPF

The proposed structure of the tri-band BPF is shown in Fig. 1. It consists of two sets of the SSLSIRs, a pair of ESIRs and two directly tapped coupling 50 Ω feed lines with the non 0°-feed coupled structure.

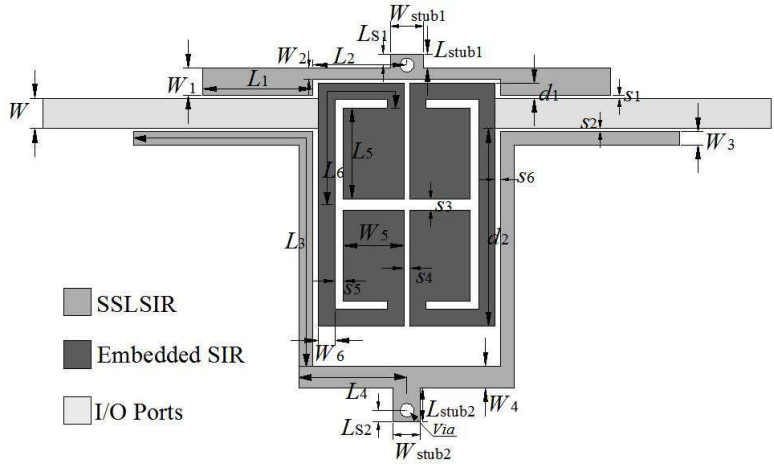

Figure 1. Schematic of the proposed tri-band BPF.

2.1. Analysis of the SSLSIR

In [10], the open stub-loaded SIR has been analyzed to design a tri-band BPF. Here, the proposed SSLSIR, a short stub-loaded section over the symmetric plane of the SIR as shown in Fig. 2(a), can be also analyzed as follows. The impedance ratio (K_1, K_2) and the length ratio (α, γ) are respectively defined as $K_1 = Z_2/Z_1$, $K_2 = Z_S/Z_1$, and $\alpha = \theta_2/(\theta_1 + \theta_2)$, $\gamma = \theta_s/(\theta_1 + \theta_2)$. The input admittance Y_{in} of the SSLSIR is derived as

$$Y_{in} = \frac{1}{Z_2} \frac{Z_1(K_1 - \tan\theta_1 \tan\theta_2) + jZ_L(K_1 \tan\theta_1 + \tan\theta_2)}{Z_L(1 - K_1 \tan\theta_1 \tan\theta_2) + jZ_1(\tan\theta_1 + K_1 \tan\theta_2)} \tag{1}$$

where $Z_L = \frac{jZ_1K_2 \tan\theta_s(\tan\theta_1 \tan\theta_2 - K_1)}{K_2 \tan\theta_s(\tan\theta_2 + K_1 \tan\theta_1) - (\tan\theta_1 \tan\theta_2 - K_1)}$. The resonant conditions of the SSLSIR will occur when $Y_{in} = 0$. By using the method of the odd- and even-mode analysis [18], the odd- and even-mode equivalent circuits are shown in Fig. 2(b) and Fig. 2(c), respectively, and the resonant condition can be expressed as follows.

The odd-mode resonances:

$$K_1 - \tan\theta_1 \tan\theta_2 = 0 \tag{2}$$

The even-mode resonances:

$$2K_2 \tan\theta_s(\tan\theta_2 + K_1 \tan\theta_1) + (\tan\theta_1 \tan\theta_2 - K_1) = 0 \tag{3}$$

From Equation (2), we can see that the odd-mode resonant condition of the SSLSIR is the same as that of the open stub-loaded SIR.

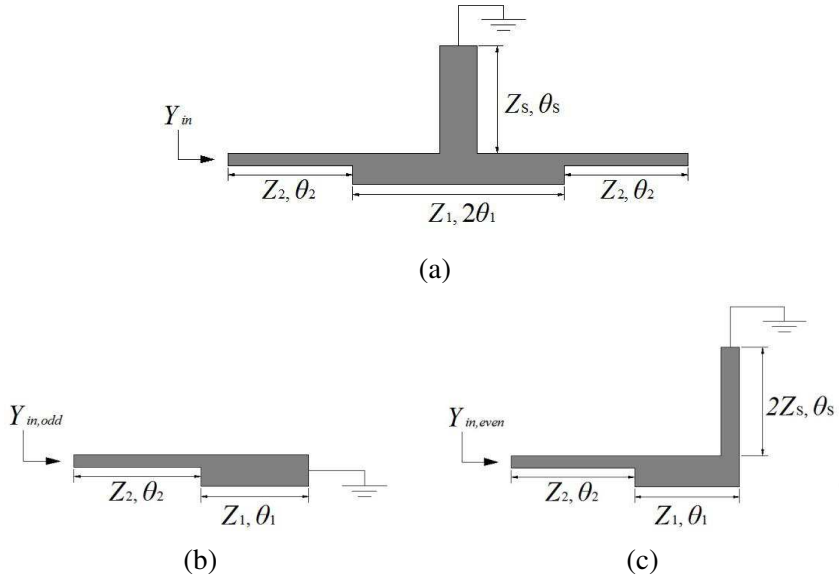

Figure 2. (a) Schematic of the proposed SSLSIR, (b) odd-mode equivalent circuit, and (c) even-mode equivalent circuit.

All of the electrical length θ_1, θ_2 and θ_s are determined for the fundamental resonant frequency f_0. Several solutions for θ_1, θ_2, and θ_s are dependent on the choice of the impedance ratio and length ratio. Compared with the conventional SIRs [11], there are more parameters to tune the distance between different resonant frequencies, thus more design freedom can be obtained. For instance, the higher resonant-frequency modes of the SSLSIR can be more easily shifted to far away or close to the fundamental resonant frequency with the help of the short stub section. Therefore, it is a great method to design a compact multi-band or wideband filter using the SSLSIR.

In this work, we use two different-dimension SSLSIRs to achieve two corresponding wide passband responses. Each of the SSLSIRs results in respective passband, and it is easy to adjust the bandwidth of each passband by changing the value γ of the corresponding SSLSIR. Fig. 3 shows the varied 3-dB bandwidths for the SSLSIRs with different impedance ratios and length ratios at 2.45 GHz and 5.2 GHz passbands, respectively. The bandwidth is increased to almost two times from around 10% to 20% when γ is varied from about 0.06 to 0.13 with $K_1 = 1.6$, $K_2 = 0.8$ and $\alpha = 0.54$ at the center frequency 2.45 GHz. While at the upper passband 5.2 GHz, as the length ratio γ increases with $K_1 = 0.4$, $K_2 = 0.33$ and $\alpha = 0.8$, the bandwidth will be

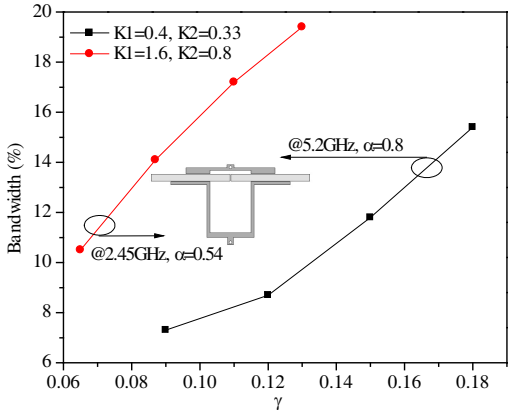

Figure 3. The 3-dB bandwidth against different length ratio γ at the lower and upper passbands separately (inset plot is the layout of dual-band filter using two different-dimension SSLSIRs).

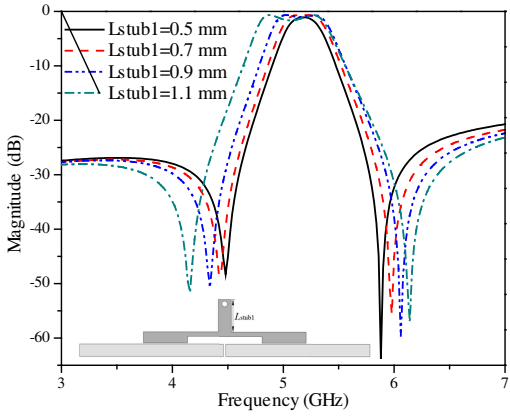

Figure 4. Frequency response of the upper passband centered at 5.2 GHz against the short stub length (inset plot is the layout of the single-band filter using a SSLSIR).

also raised. To observe the adjustable bandwidth more clearly and explicitly, we take the upper passband of the dual-band filter for instance as shown in Fig. 4. When the length of the short stub L_{stub1} increases but the other dimensions are fixed, the bandwidth will increase over a wide range. Actually, we can also obtain the same result from the lower passband.

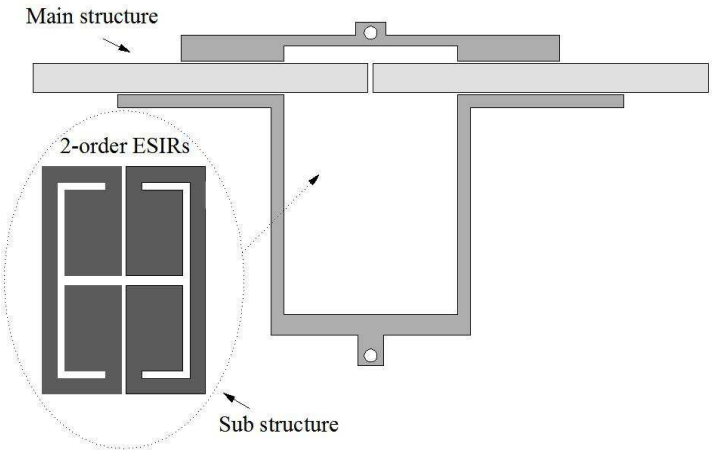

Figure 5. Structure of tri-band filter using SSLSIRs and a pair of ESIRs.

2.2. Analysis of the ESIR

Based on the above-mentioned dual-band filter using two sets of the SSLSIRs, two-order ESIRs as the sub structure are embedded into the main structure, which can be illustrated in Fig. 5. The sub filter shown in Fig. 6 consists of two conventional SIRs with directly tapped input/output (I/O) coupling. The main structure of Fig. 5 and the sub filter of Fig. 6 have the same coupling spacing s_4. In order to realize the desired coupling coefficient k of the sub filter for 3.5-GHz passband, the tap d_1 and gap s_4 of the ESIR are found to be the critical design parameter to dominate the k.

Due to the geometric limitation of the main structure, the sub filter can only employ non 0°-feed coupled structure rather than 0°-feed coupled structure [25], where no transmission zeros will appear. In this work, however, the mixed electric and magnetic coupling [26] between two SIRs are applied to obtain an extra transmission zero. Thus, the passband selectivity and stopband rejection of the filter can be effectively improved. Fig. 7 shows the S-parameter comparison of the sub filters with two different coupling styles, i.e., mixed electric and magnetic coupling, and only electric coupling.

3. RESULTS OF THE TRI-BAND FILTER

Combining two sets of SSLSIRs and a pair of ESIRs, the proposed tri-band BPF with three center frequencies at 2.45, 3.5, 5.2 GHz was

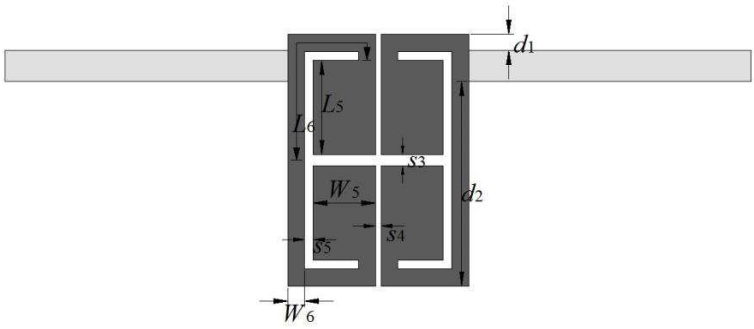

Figure 6. Structure of the sub filter using a pair of SIRs.

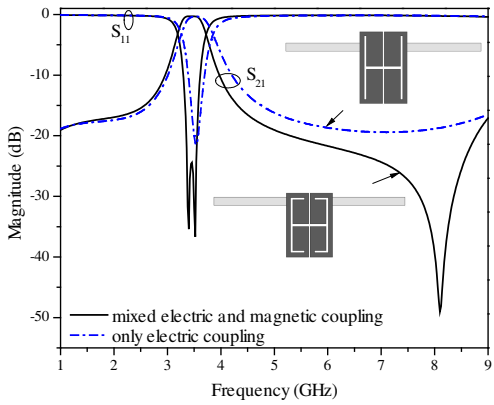

Figure 7. S-parameter comparison of the sub filters with two different coupling styles.

designed and fabricated on the RF-35 substrate with the relative dielectric constant of 3.5 and the thickness of 0.508 mm. Due to the mutual-coupling of three resonators, it is found that the 5.2 GHz passband increases in frequency, but that could be modified by the increase of the length of L_1. Finally, the parameters shown in Fig. 1 are chosen as follows: $L_1 = 4\,\text{mm}$, $L_2 = 3.4\,\text{mm}$, $L_3 = 14.5\,\text{mm}$, $L_4 = 3.9\,\text{mm}$, $L_5 = 3.3\,\text{mm}$, $L_6 = 7.2\,\text{mm}$, $L_{stub1} = 0.5\,\text{mm}$, $L_{stub2} = 1.2\,\text{mm}$, $L_{S1} = L_{S2} = 0.4\,\text{mm}$, $W = 1.1\,\text{mm}$, $W_1 = 1\,\text{mm}$, $W_2 = 0.4\,\text{mm}$, $W_3 = 0.5\,\text{mm}$, $W_4 = 0.8\,\text{mm}$, $W_5 = 2.2\,\text{mm}$, $W_6 = 0.6\,\text{mm}$, $W_{stub1} = 1.2\,\text{mm}$, $W_{stub2} = 1\,\text{mm}$, $s_1 = s_2 = 0.1\,\text{mm}$, $s_3 = 0.4\,\text{mm}$, $s_4 = 0.2\,\text{mm}$, $s_5 = 0.3\,\text{mm}$, $d_1 = 0.55\,\text{mm}$, $d_2 = 7.15\,\text{mm}$. The diameter dimensions of via holes in two SSLSIRs are both chosen 0.5 mm. The

characteristic impedance of the input/output microstrip is taken as 50 Ohm.

Figure 8 depicts the current density at three resonant frequencies. In Fig. 8(a), the first resonance created by one SSLSIR generates a RF signal path from source to load. In this case, the other SSLSIR and the ESIRs do not resonate, so they do not affect the response of the first passband. Similarly, as shown in Fig. 8(b) and Fig. 8(c), the other two RF signal paths are generated by the other SSLSIR and ESIRs respectively, to obtain the second and third passbands. Each passband can be implemented individually, and good selectivity and low insertion loss of the each passband can be well achieved.

The simulation and measurement are accomplished by the high frequency structural simulator (HFSS) and 8757D network analyzer, respectively. Both measured and simulated results are plotted in Fig. 9. As can be seen from Fig. 9, the filter has three passbands centered at 2.45, 3.5 and 5.2 GHz with 3-dB bandwidths of 235 MHz (9.6%), 458 MHz (13.1%) and 410 MHz (7.9%), respectively. The insertion losses, including the losses from two SMA connectors, are 1.2, 1.5 and 1.6 dB at 2.45, 3.5 and 5.2-GHz passbands, respectively. While the return losses within the three passbands are better than 12.9 dB. The measured results are in good agreement with the full-wave simulated

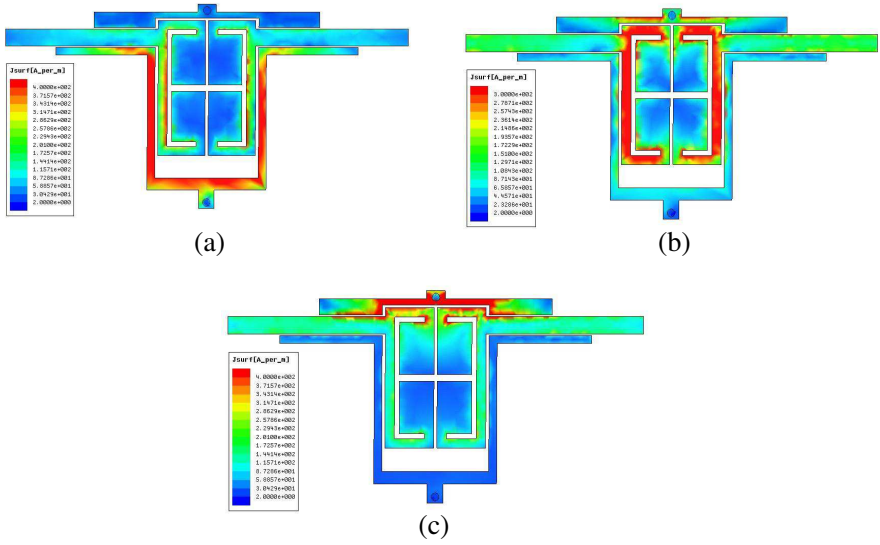

Figure 8. Simulated electric current density. (a) First resonance 2.45 GHz, (b) second resonance 3.5 GHz, and (c) third resonance 5.2 GHz.

ones. Slight deviation is observed, which could be attributed to fabrication tolerance in the implementation. Its size only amounts to $13.3\,\text{mm} \times 19.8\,\text{mm}$ ($0.18\lambda_g \times 0.27\lambda_g$, where λ_g is the guided wavelength of 50 Ohm microstrip at the center frequency of the first passband). Table 1 summarizes the comparisons of the proposed filter with other reported tri-band filters in recent years. It demonstrates that this work has realized miniaturization and improved selectivity with wide band. Fig. 10 shows the photograph of the fabricated filter.

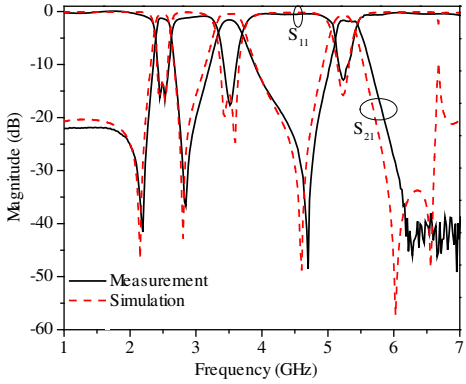

Figure 9. Simulated and measured frequency response of the filter.

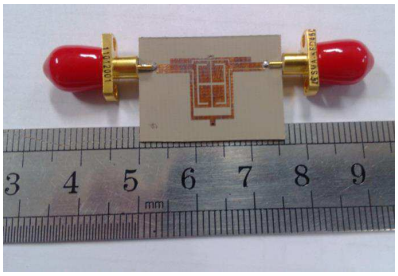

Figure 10. Photograph of the fabricated BPF.

Table 1. Performance comparison of some reported tri-band bandpass filters.

Reference	ε_r/h (mm) of substrate	Three passbands (GHz)	Return loss (dB)	Insert loss (dB)	3-dB FBW (%)	Circuit size (mm^2) ($\lambda_g \times \lambda_g$)
[1]	2.45/0.79	1.51/4 /6.26	11/28/24	2.5/1.6 /2.5	4.1/3.4 /2.3	26×26 (0.19×0.19)
[7]	10.8/1.27	2.35/4.78 /7.21	17/21/16	1.78/0.9 /0.7	5.31/6.27 /8.66	about 20×20 (0.42×0.42)
[10]	2.2/0.787	1.575/2.4 /3.5	9/18.9 /13.5	1.6/1.5 /2.3	5.2/3.8 /4.6	49.7×56.2 (0.36×0.40)
[16]	2.2/0.787	1.8/2.7 /3.3–4.8	14/13/9	2.2/2.1 /1.3	3.9/2.6 /40	37.5×27.8 (0.33×0.25)
This work	3.5/0.508	2.45/3.5 /5.2	16.3/17.9 /12.9	1.2/1.5 /1.6	9.6/13.1 /7.9	13.3×19.8 (0.18×0.27)

4. CONCLUSION

In this paper, a simple and effective approach to design a low-loss miniaturized tri-band filter based on SSLSIRs and ESIRs is presented. The proposed filter is designed to meet the specifications at the first passband of 2.45 GHz, at the second passband of 3.5 GHz, and at the third passband of 5.2 GHz. The new SSLSIRs possess the advantage of adjustable bandwidths, and the ESIRs employ non 0°-feed coupled structure with mixed electric and magnetic coupling to obtain an extra transmission zero. Moreover, the embedded resonators structure can further miniaturize the dimensions of the overall structure. The simulated and measured results show that the proposed compact filter has the advantage of tri-band response, low insertion loss, high skirt selectivity and low cost for WLAN and WiMAX applications.

ACKNOWLEDGMENT

This work was partially supported by the China Scholarship Council (CSC) and partially by a project (No. IRT1113) under "Program for Changjiang Scholars and Innovation Team in University".

REFERENCES

1. Li, X. and H. Wang, "An approach for multi-band bandpass filter design based on asymmetric half-wavelength resonators," *Progress In Electromagnetics Research*, Vol. 140, 31–42, 2013.
2. Chen, C.-Y., C.-Y. Hsu, and H.-R. Chuang, "Design of miniature planar dual-band filter using dual-feeding structures and embedded resonators," *IEEE Microw. Wirel. Compon. Lett.*, Vol. 16, No. 12, 669–671, 2006.
3. Kuo, J.-T. and S.-W. Lai, "New dual-band bandpass filter with wide upper rejection band," *Progress In Electromagnetics Research*, Vol. 123, 371–384, 2012.
4. Luo, X., H.-Z. Qian, J.-G. Ma, K.-X. Ma, and K. S. Yeo, "Compact dual-band bandpass filters using novel embedded spiral resonator (ESR)," *IEEE Microw. Wirel. Compon. Lett.*, Vol. 20, No. 8, 435–437, 2010.
5. Xu, K.-D., Y.-H. Zhang, C.-L. Zhuge, and Y. Fan, "Miniaturized dual-band bandpass filter using short stub-loaded dual-mode resonators," *Journal of Electromagnetic Waves and Applications*, Vol. 25, No. 16, 2264–2273, 2011.
6. Yang, C.-F., Y.-C. Chen, C.-Y. Kung, J.-J. Lin, and T.-P. Sun, "Design and fabrication of a compact quad-band bandpass filter

using two different parallel positioned resonators," *Progress In Electromagnetics Research*, Vol. 115, 159–172, 2011.

7. Xiao, J.-K. and W.-J. Zhu, "Compact split ring SIR bandpass filters with dual and tri-band," *Progress In Electromagnetics Research C*, Vol. 25, 93–105, 2012.
8. Wu, H.-W. and R.-Y. Yang, "A new quad-band bandpass filter using asymmetric stepped impedance resonators," *IEEE Microw. Wirel. Compon. Lett.*, Vol. 21, No. 4, 203–205, 2011.
9. Hu, J. P., G. H. Li, H. P. Hu, and H. Zang, "A new wideband triple-band filter using SIR," *Journal of Electromagnetic Waves and Applications*, Vol. 25, No. 16, 2287–2295, 2011.
10. Chen, W.-Y., M.-H. Weng, and S.-J. Chang, "A new tri-band bandpass filter based on stub-loaded step-impedance resonator," *IEEE Microw. and Wirel. Compon. Lett.*, Vol. 22, No. 4, 179–181, 2012.
11. Makimoto, M. and S. Yamashita, "Compact bandpass filters using stepped impedance resonators," *Proceedings of the IEEE*, Vol. 67, No. 1, 16–19, 1979.
12. Wei, X. B., Y. Shi, P. Wang, J. X. Liao, Z. Q. Xu, and B. C. Yang, "Design of compact, wide stopband bandpass filter using stepped impedance resonator," *Journal of Electromagnetic Waves and Applications*, Vol. 26, Nos. 8–9, 1095–1104, 2012.
13. Hsu, C.-I.-G., C.-H. Lee, and Y.-H. Hsieh, "Tri-band bandpass filter with sharp passband skirts designed using tri-section SIRs," *IEEE Microw. Wirel. Compon. Lett.,* Vol. 18, 19–21, 2008.
14. Liu, S.-K. and F.-Z. Zheng, "A new compact tri-band bandpass filter using step impedance resonators with open stubs," *Journal of Electromagnetic Waves and Applications*, Vol. 26, No. 1, 130–139, 2012.
15. Ma, D., Z. Y. Xiao, L. Xiang, X. Wu, C. Huang, and X. Kou, "Compact dual-band bandpass filter using folded SIR with two stubs for WLAN," *Progress In Electromagnetics Research*, Vol. 117, 357–364, 2011.
16. Chen, W.-Y., M.-H. Weng, S.-J. Chang, H. Kuan, and Y.-H. Su, "A new tri-band bandpass filter for GSM, WiMAX and ultra-wideband responses by using asymmetric stepped impedance resonators," *Progress In Electromagnetics Research*, Vol. 124, 365–381, 2012.
17. Weng, M.-H., C.-H. Kao, and Y.-C. Chang, "A compact dual-band bandpass filter with high band selectivity using cross-coupled asymmetric SIRs for WLANs," *Journal of Electromagnetic Waves*

and Applications, Vol. 24, Nos. 2–3, 161–168, 2011.

18. Zhang, X. Y., J. X. Chen, Q. Xue, and S. M. Li, "Dual-band bandpass filter using stub-loaded resonators," *IEEE Microw. Wirel. Compon. Lett.*, Vol. 17, No. 8, 583–585, 2007.
19. Chen, F.-C., Q.-X. Chu, and Z.-H. Tu, "Design of compact dual-band bandpass filter using short stub loaded resonator," *Microw. Opt. Technol. Lett.*, Vol. 51, No. 4, 959–963, 2009.
20. Zhou, M., X. Tang, and F. Xiao, "Compact dual band bandpass filter using novel E-type resonator with controllable bandwidth," *IEEE Microw. Wirel. Compon. Lett.*, Vol. 18, No. 12, 779–781, 2008.
21. Tu, W.-H. and K. Chang, "Miniaturized dual-mode bandpass filter with harmonic control," *IEEE Microw. Wirel. Compon. Lett.*, Vol. 15, No. 12, 838–840, 2005.
22. Chen, F. C., Q. X. Chu, and Z. H. Tu, "Tri-band bandpass filter using stub loaded resonators," *Electron. Lett.,* Vol. 44, 747–749, 2008.
23. Wei, C. L., B. F. Jia, and Z. J. Zhu, "Design of different selectivity dual-mode filters with E-shaped resonator," *Progress In Electromagnetics Research*, Vol. 116, 517–532, 2011.
24. Deng, H.-W., Y.-J. Zhao, Y. Fu, X.-J. Zhou, and Y.-Y. Liu, "Design of tri-band microstrip BPF using SLR and quarter-wavelength SIR," *Microw. Opt. Technol. Lett.,* Vol. 55, 212–215, 2013.
25. Tsai, C.-M., S.-Y. Lee, and C.-C. Tsai, "Performance of a planar filter using a 0° feed structure," *IEEE Trans. Microw. Theory Tech.*, Vol. 50, 2362–2367, 2002.
26. Chu, Q.-X. and H. Wang, "A compact open-loop filter with mixed electric and magnetic coupling," *IEEE Trans. Microw. Theory Tech.*, Vol. 56, 431–439, 2008.